

Sublimation of a heavily boron-doped Si(111) surface

Yoshikazu Homma,* Hiroki Hibino, and Toshio Ogino
NTT Basic Research Laboratories, Atsugi, Kanagawa 243-0198, Japan

Noriyuki Aizawa
Tokyo Gakugei University, Koganei, Tokyo 184-8501, Japan
 (Received 29 June 1998)

We investigated sublimation of a heavily boron-doped Si(111) surface in comparison with that of a normal Si(111) surface in ultrahigh vacuum. Step spacing during step-flow sublimation is analyzed as a measure of the adatom diffusion length using $>50\text{-}\mu\text{m}$ -wide (111) planes created at the bottom of craters. On the heavily doped 1×1 surface, the step spacing is smaller and the step-spacing transition (or “incomplete surface melting” transition) temperature is 60° higher than those on the normal 1×1 surface. These results are interpreted in terms of the effect of boron at S_5 substitutional sites. Below 1100°C , the sublimation of heavily doped surface on the wide terrace turns into a two-dimensional vacancy-island nucleation mode from step-flow sublimation observed above 1100°C . [S0163-1829(98)05243-6]

I. INTRODUCTION

Sublimation of surfaces is the reverse process of epitaxial growth in the sense that adatoms are released from steps and desorb from the surface. However, sublimation also involves pair formation or annihilation of an adatom and an vacancy so it is a more complicated process than growth. On silicon surface, sublimation basically takes place in a step-flow manner. All steps flow in the same direction, which keeps the vicinality of the substrate. The phenomena relating to sublimation, however, appear different for Si(001) and Si(111) in the high-temperature regime. On Si(001) surfaces, step flow breaks down, and macrovacancy (monolayer-deep hole) formation has been observed on micrometer-scale terraces.¹⁻³ At around 1180°C , the density of holes is so high that surface roughening occurs and steps become invisible. On the other hand, step-flow sublimation continues up to very high temperatures on Si(111).^{4,5} This different behavior between Si(001) and Si(111) is primarily due to the difference in adatom diffusion length; the diffusion length on Si(111) is one order of magnitude larger than on Si(001). In addition, the diffusion of adatoms and vacancies is anisotropic relative to the dimer-row direction on Si(001), which cause the further complication of different behavior between the two types of steps, i.e., steps parallel to the dimer rows and those perpendicular to the dimer rows. Recently, a tensile strain induced by dopant segregation was found to protract step flow up to a higher temperature on Si(001).⁶

For the investigation of macrovacancy formation on Si(111), a terrace larger than $20\ \mu\text{m}$ is necessary. We have accomplished such observation using a huge (111) plane at the bottom of crater formed on a vicinal Si(111) surface.⁷ At the crater bottom, atomic steps retract in a step-flow manner, which causes the very bottom terrace to expand.⁸ Macrovacancy formation was observed at the center of the terrace when the terrace size became wide enough. This process determined step spacing on the bottom plane of the crater. In addition, a transitionlike increase in the step spacing was found at 1200°C .⁷ We assumed this transition was “incom-

plete surface melting,” which is a disordering of the first monolayer. Quite recently, Hibino *et al.* confirmed this assumption using reflection high-energy electron diffraction and medium-energy ion-scattering spectroscopy.⁹

In this paper, we focus on sublimation of heavily boron-doped Si(111). Upon annealing, boron segregates to the surface, which then exhibits a $\sqrt{3}\times\sqrt{3}$ reconstruction.¹⁰ Therefore, the sublimation phenomena should be different from those on a normal Si(111) surface. Even after the disappearance of $\sqrt{3}\times\sqrt{3}$ structure at a high temperature, boron is expected to influence sublimation phenomena. We compare the step spacing and the step-spacing transition (incomplete surface melting transition) between heavily boron-doped and normal (111) surfaces by using wide terraces created at the bottom of craters. We show the peculiar behaviors of the heavily boron-doped surface.

II. EXPERIMENT

A heavily boron-doped Si(111) wafer ($\sim 0.001\ \Omega\text{cm}$) 0.3° miscut from the (111) plane was used as the substrate. Specimens of $5\times 15\ \text{mm}^2$ were cut from the wafer. The long side of each specimen was nearly parallel to the miscut orientation, the $[11\bar{2}]$ direction. A lightly boron-doped wafer ($\sim 5\ \Omega\text{cm}$) 0.15° miscut was used for comparison. The long side of the specimens cut from this wafer was parallel to the miscut orientation, $[2\bar{1}\bar{1}]$. Square craters with sides of $150\times 150\ \mu\text{m}^2$ and a depth of about $1\ \mu\text{m}$ were formed on the surfaces by O_2^+ beam raster scanning with a secondary-ion-mass spectrometry instrument. The beam energy was $10.5\ \text{keV}$, and the beam diameter was about $30\ \mu\text{m}$. The specimens were then repeatedly oxidized using a $\text{H}_2\text{SO}_4:\text{H}_2\text{O}_2$ (4:1) solution, and etched using dilute HF for several cycles to remove possible contamination caused by the crater formation process. After the final oxidation cycle, they were introduced into an ultrahigh-vacuum scanning electron microscope (UHV-SEM) (Refs. 11 and 12), and resistively heated using direct current. The temperature was measured with an infrared pyrometer, which was calibrated using a

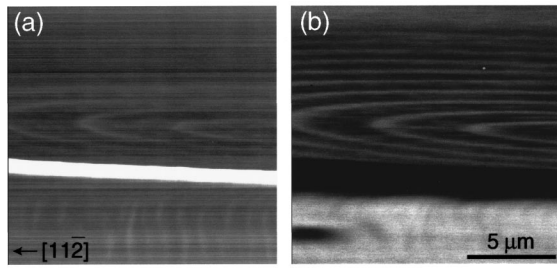


FIG. 1. SEM (a) and SREM (b) images of the crater bottom on the heavily boron-doped Si(111) surface. The surface was quenched from 1220 °C. The SREM image was produced using one of the $\sqrt{3} \times \sqrt{3}$ diffraction spots.

disappearance filament pyrometer, taking into consideration the temperature dependence of the emissivity.¹³ The heating power dependence of the temperature followed exactly the same curve above 1100 °C for the two types of substrates, indicating that the high concentration of boron did not affect emissivity. Since the specimens were clamped using tantalum foil spacers with uniform force, the temperature was uniform in the central region, and the reproducibility of the temperature was quite high. Nevertheless, we estimate the accuracy of temperature measurements as $\pm 20^\circ$ for around 1200 °C.

The step distribution was observed *in situ* in the UHV-SEM. To make the atomic step observation easier (see Sec. II), we radiation quenched the surface by turning off the heating current. The cooling rate was about 150 °C/s from above 1200 °C to 600 °C.

III. RESULTS

A. Step distribution on sublimating terrace

In our previous work using a normal Si(111) surface, we decorated atomic steps with a 7×7 structure on a planarized surface by radiation quenching the surface.⁷ On the quenched surface, continuous 7×7 regions nucleated at steps, thus steps appeared as brighter lines in an SEM image. A heavily boron-doped Si(111) surface exhibits a $\sqrt{3} \times \sqrt{3}$ reconstruction up to 1100 °C. The 7×7 reconstruction never appears on this surface. However, atomic steps on a planarized surface can be imaged by quenching the sample from a higher temperature. Figure 1 shows a SEM and a scanning reflection electron microscopy (SREM) image of the bottom of a crater on the heavily boron-doped Si(111). The SREM image was produced using a reflection high-energy electron-diffraction spot from the $\sqrt{3} \times \sqrt{3}$ structure. Both images show concentric circles similar to those in a planarized area on a normal (111) surface (as seen in Fig. 1 in Ref. 7). This means that the $\sqrt{3} \times \sqrt{3}$ structure also nucleates from steps and cannot expand to cover the whole surface during rapid quenching. Therefore, the steps on the heavily boron-doped (111) surface can be visualized by the SEM in just the same way as the 7×7 decoration.

The surface images of the heavily boron-doped Si(111) exhibit three different features, depending on the temperature from which the sample is quenched. Figure 2 shows typical images for each temperature region. Figures 2(b) and 2(c) are similar to those of a normal Si(111) surface. Figure 2(b)

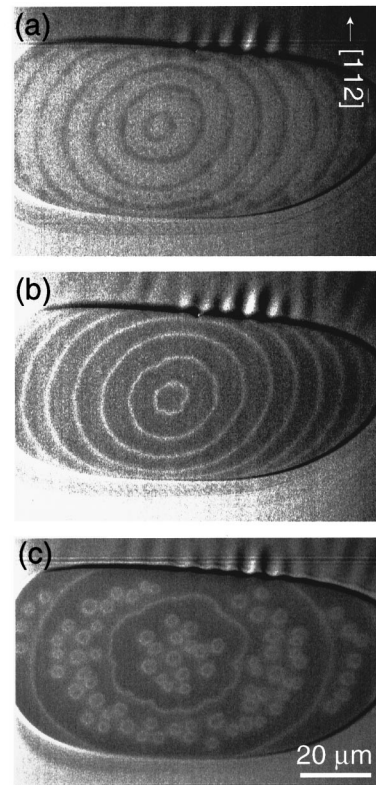


FIG. 2. SEM images showing temperature-dependent step distributions on a wide (111) plane formed on the heavily boron-doped Si(111) substrate. Images were taken after quenching from (a) 1040, (b) 1230, and (c) 1270 °C. Continuous $\sqrt{3} \times \sqrt{3}$ domains nucleated at steps during quenching, and appear brighter than the rest of the surface.

shows step distribution in a concentric circular shape, which is a characteristic of a wide terrace sublimating in a step-flow manner. Figure 2(c) corresponds to the step distribution of an incompletely melted surface. The step spacing is tripled compared to Fig. 2(b), and small circular steps can be seen. These small circular steps are formed in between concentric circular steps during the quenching process.

Of interest is Fig. 2(a), which was obtained below the $1 \times 1 - \sqrt{3} \times \sqrt{3}$ transition temperature (1100 °C). The contrast in the SEM image is reversed with respect to Fig. 2(b). This contrast inversion is due to vacancy island formation on the terraces. Successive images taken during heating clarify the phenomenon occurring. The images in Fig. 3 were obtained after repeatedly heating and quenching. The initial surface was prepared by quenching from 1220 °C, then the sample was heated to 1056 °C. The contrast inverts in the early stage, and stays inverted up until 70 s of heating. Then it returns to one similar to the initial one. This contrast change is repeated upon further heating. The step shapes remain almost the same throughout this cycle.

This phenomenon is interpreted as layer-by-layer sublimation with monolayer vacancy-island formation. The SEM image remains the same even when the area of vacancy islands increases during sublimation, because the $\sqrt{3} \times \sqrt{3}$ area nucleated during quenching is larger than the vacancy islands. However, upon 1-ML sublimation, the surface smoothens again, resulting in contrast recovery. During the contrast inversion period, darker zones are seen just near

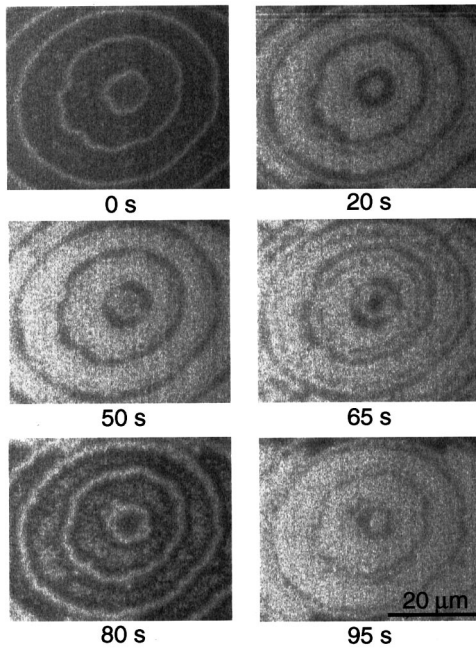


FIG. 3. SEM contrast change during sublimation of a wide (111) plane on the heavily boron-doped Si(111) at 1056 °C. The initial surface (0 s) was prepared by quenching from 1220 °C. Images were then taken by repeatedly heating and quenching. The cumulative heating time is shown below each image.

steps. These are denuded zones where no vacancy island exists due to the steps acting as sinks for vacancies. Though the width of a denuded zone is larger for a lower trace than for an upper terrace (steps descend toward the center of the planarized region), it is on the order of several μm and much smaller than the terrace size. This indicates that the vacancy (or adatom) diffusion length on the $\sqrt{3} \times \sqrt{3}$ surface becomes smaller than that on the 1×1 surface, resulting in a sublimation mode change from step flow to two-dimensional island formation in a wide terrace. The width of the denuded zone showed very little temperature dependence at 1000–1100 °C.

It is strange enough that the $\sqrt{3} \times \sqrt{3}$ decoration of steps is still seen on a wide terrace even below the $1 \times 1 - \sqrt{3} \times \sqrt{3}$ transition temperature. However, this contrast around steps cannot be observed below 1000 °C. We speculate that the $\sqrt{3} \times \sqrt{3}$ structure may be imperfect on a terrace wider than the diffusion length of a vacancy (or adatom) in the temperature range of 1000–1100 °C, and a well-ordered $\sqrt{3} \times \sqrt{3}$ structure is only formed near the steps during quenching.

The step spacing on the wide terrace changes depending on temperature above 1100 °C. The average step spacing between the first and second concentric circles was derived at each temperature for the heavily boron-doped Si(111), and the results are plotted in Fig. 4. For comparison, the data for a lightly boron-doped Si(111) are also plotted. The step spacing of the heavily doped sample exhibits a temperature dependence similar to that of the lightly doped sample with a step-spacing transition. However, the transition temperature of the heavily doped sample is about 60° higher than that of the lightly doped one. Furthermore, the step spacing is smaller for the heavily doped sample below the transition temperature. Above the transition temperature, the step spac-

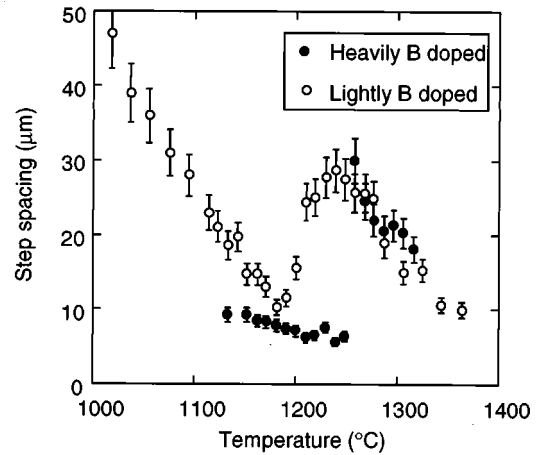


FIG. 4. Temperature dependence of step spacing on the heavily boron-doped Si(111) surface and lightly boron-doped Si(111) surface.

ing is almost the same for both samples. Here it should be noted that the effect of electric current on step bunching changes at around the transition temperature on the heavily doped surface, just as on a lightly doped surface.⁷ The step bunching was induced with a step-down current above 1260 °C, and with a step-up current below 1260 °C (but above 1100 °C).

B. Sublimation rate

The sublimation rate of the heavily boron-doped sample can be precisely determined from the period of contrast change, such as shown in Fig. 3, in the temperature range from 1000 to 1100 °C. The period corresponds exactly to the sublimation of one bilayer (1.6×10^{15} atoms/cm²). For the lightly boron-doped sample, the sublimation rate was derived from step retraction velocity on a wide terrace at various temperatures. The results are shown in Fig. 5, where previously reported values (Refs. 5, 14, and 15) are also plotted.

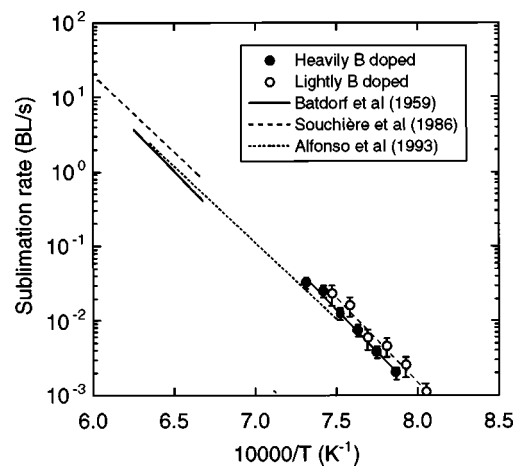


FIG. 5. Arrhenius plot of sublimation rate (bilayer/s) for the heavily boron-doped Si(111) surface and lightly boron-doped Si(111) surface. The heavily doped data were derived from the period of SEM contrast change, such as shown in Fig. 3, while the lightly doped data were obtained from the step retraction rate. Curves from Refs. 5, 14, and 15 are also shown.

The sublimation rates for both samples agree within the experimental error, and they are consistent with the values measured at higher temperatures in the literature. Although we could not accurately measure the sublimation rate for a higher temperature range, we assume that it depends very little on the boron concentration above 1100 °C. This is realistic because even the sublimation rate of the $\sqrt{3} \times \sqrt{3}$ surface is almost the same as a normal 1×1 surface. It should be noted that the sublimation rate shows no anomaly at the step-spacing transition temperature.

VI. DISCUSSION

The decrease in step spacing with increasing in temperature has been explained by adatom desorption.⁷ The desorption of adatoms increases with temperature, which causes macrovacancy formation in the center of the bottom terrace. The bases of the phenomena were treated by Pimpinelli and Villain based on the Burton, Cabrera, and Frank theory (Ref. 16), taking into account advacancy formation.¹⁷ They showed that macrovacancies nucleate on an evaporating vicinal surface when the step-step spacing ℓ roughly satisfies (atomic spacing as unit length)

$$\frac{8\pi\gamma^2}{(\kappa\ell/kT)^2} < 2 \ln \ell, \quad (1)$$

where γ is the step stiffness, k is the Boltzmann constant, T is the absolute temperature, and

$$\kappa^2 = \frac{\rho_0/\tau_v}{D\rho_0 + \Lambda\sigma_0}, \quad (2)$$

where ρ_0 and σ_0 are the equilibrium adatom and advacancy densities, respectively, D and Λ are the adatom and advacancy diffusion coefficients, respectively, and τ_v is the adatom lifetime before desorption. In the present case $\ell \approx 10^4$ nm (or 10^5 atomic spacing), and we can reasonably assume $D\rho_0 \gg \Lambda\sigma_0$, so

$$\kappa^2 \approx 1/(D\tau_v) = 1/\lambda_s^2, \quad (3)$$

where λ_s is the adatom diffusion length before desorption. Thus inequality (1) gives

$$\ell > \lambda_s \gamma / kT. \quad (4)$$

On the (111) surface, γ is of the order of kT (although the measured dynamical step stiffness showed a large variation with temperature; see Ref. 18). Thus inequality (4) implies that macrovacancies nucleate when the terrace size is of the order of the adatom diffusion length. Pimpinelli and Villain's model is for a terrace between two parallel steps. In the present case, the bottom terrace is circular. A simple calculation shows that the adatom concentration at the center of the circular bottom terrace with radius ℓ is $\frac{1}{2}$ that of a staircase terrace with width 2ℓ . In spite of this difference, the criterion for macrovacancy nucleation expressed by inequality (4) can be used as a rough estimation: macrovacancies nucleate when the radius of the terrace becomes larger than the order of the adatom diffusion length, and then step flow is maintained without macrovacancy formation until the next

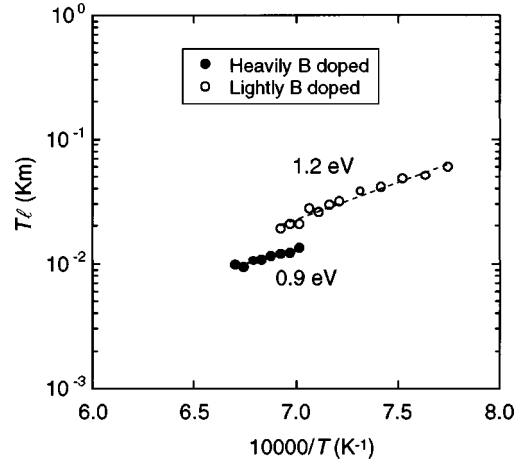


FIG. 6. Arrhenius plot of step spacing multiplied by absolute temperature for the data below the step-spacing transition. Data for the heavily boron-doped Si(111) surface and lightly boron-doped Si(111) surface are compared.

step appears in the center of the terrace. Therefore, the step spacing in Fig. 4 follows the temperature dependence of the adatom diffusion length.

Since $\lambda_s = a \exp[(W_v - W_{sd})/2kT]$, where a is the atomic spacing, W_v is the desorption barrier for adatoms, and W_{sd} is the surface diffusion barrier for adatoms,¹⁷

$$\ell \approx (\gamma/kT)a \exp[(W_v - W_{sd})/2kT]. \quad (5)$$

Hence, the Arrhenius plot of $T\ell$ vs $1/T$ gives $(W_v - W_{sd})/2$ as the activation energy, and γ as the prefactor. The plot is shown in Fig. 6, and it yields an activation energy of $W_v - W_{sd} = 2.4$ eV for the lightly boron-doped Si(111), and 1.8 eV for the heavily-doped Si(111). The γ values are 0.4 ± 0.2 and 3 ± 2 eV/Å for lightly and heavily doped samples, respectively. These are within the reported dynamical step-stiffness values for Si(111),¹⁸ but they are not reliable enough. Since the prefactor is determined by the intersection with the ordinate of the Arrhenius plot based on a small $1/T$ region, a small difference in the plot slope (i.e., the activation energy) can cause a large error in γ .

The sublimation rate is expressed by

$$v = v_o \exp[-(W_v + W_a)/kT], \quad (6)$$

where v_o is the atomic frequency and W_a is the adatom formation energy. The results in Fig. 5 indicate that $W_v + W_a$ (~ 4.3 eV) barely change for the heavily doped and lightly doped samples. At first sight, this may be hard to understand, because W_a should be different for $\sqrt{3} \times \sqrt{3}$ and 1×1 surfaces. However, W_a on the 1×1 surface is about 0.2 eV (i.e., $W_v \gg W_a$).¹⁷ It is also expected for the $\sqrt{3} \times \sqrt{3}$ surface that $W_v \gg W_a$. Hence the results in Fig. 5 mean that W_v is almost the same for the heavily doped and lightly doped samples. Then the difference in $W_v - W_{sd}$ between the heavily doped and lightly doped 1×1 surfaces is reduced to the difference in W_{sd} . That is, the adatom diffusion barrier for the heavily doped 1×1 surface is 0.6 eV higher than that for the lightly doped 1×1 surface.

The reason for the higher diffusion barrier might be the influence of boron at subsurface sites. It is well established

that boron atoms are located at substitutional S_5 sites in the second layer, and stabilize T_4 site adatoms on a $\sqrt{3} \times \sqrt{3}$ -B surface.¹⁹ Above 1100 °C the surface does not retain the $\sqrt{3} \times \sqrt{3}$ reconstruction any longer. However, we speculate that some boron atoms still remain at S_5 sites at temperatures between 1100 and 1260 °C. This is verified by the high activation energy (3.5 eV) of exchange between B and Si atoms on a $\sqrt{3} \times \sqrt{3}$ surface.²⁰ It follows then that the lifetime of adatoms staying at T_4 sites may be longer, although adatoms do not stay still at T_4 sites. The longer lifetime would make the adatom diffusion barrier higher. In addition, it could contribute to increase the step stiffness and make the incomplete melting transition temperature higher. After the incomplete melting transition, which is the disordering of the first monolayer,²¹ boron atoms do not locate at the subsurface sites, so the surface property should be the same as that of the lightly doped surface. This would explain the same step spacing for both samples after the incomplete melting transition.

The occurrence of vacancy-island-nucleation-mode sublimation below 1100 °C is puzzling. In the scheme of inequality (4), this means a decrease of the adatom diffusion length to several μm . On a $\sqrt{3} \times \sqrt{3}$ -B surface, T_4 adatoms form the $\sqrt{3} \times \sqrt{3}$ structure, and their hopping probably is low. However, non- T_4 adatoms can diffuse on the $\sqrt{3} \times \sqrt{3}$ structure. Deposited Si atoms are reported to be very mobile on a $\sqrt{3} \times \sqrt{3}$ -B surface.²² This contradicts the lower-diffusion-length picture. One explanation for this is that the density of non- T_4 adatoms is so small, (i.e., a larger W_a) on the $\sqrt{3} \times \sqrt{3}$ surface that T_4 adatoms play the major role in the adatom diffusion and advacancy creation in inequality (1). In this situation, the diffusion barrier of a T_4 adatom and, in turn, that of an advacancy, is high because of the closely

packed T_4 adatom configuration. In contrast, a non- T_4 adatom can diffuse to a step or evaporate easily. (We might be able to assume a low W_v , although this could contradict our previous assumption of $W_v \gg W_a$). Hence, the density of advacancies exceeds that of non- T_4 adatoms, which causes a high macrovacancy density on a wide terrace. Our finding that the denuded zone width is independent of temperature on the $\sqrt{3} \times \sqrt{3}$ surface suggests $W_v - W_{sd} \approx 0$. This also can be interpreted as a consequence of the low mobility of T_4 adatoms.

V. CONCLUSIONS

We investigated sublimation of a heavily boron-doped Si(111) surface in comparison with that of a normal Si(111) surface using SEM observations of step distribution on wide (111) planes created at the bottom of craters. Steps on the wide (111) plane were decorated with a $\sqrt{3} \times \sqrt{3}$ structure after quenching; thus they could be imaged by SEM. The step spacing on the plane depends on the heating temperature, and reflects the adatom diffusion length. The step spacing on the heavily doped 1×1 surface is smaller than that on the normal 1×1 surface. In addition, the incomplete surface melting transition of the heavily doped surface occurred 60° higher than that of the normal 1×1 surface, 1200 °C. These were attributed to the segregation of boron, some of which might stay at S_5 sites even in the 1×1 phase above 1100 °C, and reduce the adatom diffusion length. It might possibly increase the step stiffness, resulting in the higher incomplete melting transition temperature. We also found that the sublimation mode changes from a step-flow to a two-dimensional vacancy-island nucleation on the wide terrace of the heavily doped surface below 1100 °C. This might be due to a low mobility of T_4 adatoms on the $\sqrt{3} \times \sqrt{3}$ -B surface.

*Electronic address: homma@will.brl.nntt.co.jp

¹J. J. Métois and D. E. Wolf, Surf. Sci. **298**, 71 (1993).

²M. Mundschau, E. Bauer, W. Teliéps, and W. Świech, Surf. Sci. **223**, 413 (1989).

³A. Pimpinelli and J. J. Métois, Phys. Rev. Lett. **72**, 3566 (1994).

⁴A. V. Latyshev, A. L. Aseev, A. B. Krasilnikov, and S. I. Stenin, Surf. Sci. **213**, 157 (1989).

⁵C. Alfonso, J. C. Heyraud, and J. J. Métois, Surf. Sci. Lett. **291**, L745 (1993).

⁶C. M. Roland, M. G. Wensell, Y. Hong, and I. S. T. Tson, Phys. Rev. Lett. **78**, 2608 (1997).

⁷Y. Homma, H. Hibino, T. Ogino, and N. Aizawa, Phys. Rev. B **55**, R10 237 (1997).

⁸Y. Homma, T. Ogino, and N. Aizawa, Jpn. J. Appl. Phys., Part 2 **35**, L241 (1996).

⁹H. Hibino, K. Sumitomo, T. Fukuda, Y. Homma, and T. Ogino Phys. Rev. B (to be published).

¹⁰V. V. Korobtsov, V. G. Lifshits, and A. V. Zotov, Surf. Sci. **195**, 466 (1988).

¹¹Y. Homma, M. Tomita, and T. Hayashi, Surf. Sci. **258**, 147 (1991); Ultramicroscopy **52**, 187 (1993).

¹²Y. Homma, M. Suzuki, and M. Tomita, Appl. Phys. Lett. **62**, 3276 (1993).

¹³F. G. Allen, J. Appl. Phys. **28**, 1510 (1957).

¹⁴R. L. Batdorf and F. M. Smits, J. Appl. Phys. **30**, 259 (1959).

¹⁵J. L. Souchière and VU. Thien Binh, Surf. Sci. **168**, 52 (1986).

¹⁶W. K. Burton, N. Cabrera, and F. C. Frank, Philos. Trans. R. Soc. London, Ser. A **243**, 299 (1951).

¹⁷A. Pimpinelli and J. Villain, Physica A **204**, 521 (1994).

¹⁸A. V. Latyshev, H. Minoda, Y. Tanishiro, and K. Yagi, Phys. Rev. Lett. **76**, 94 (1996).

¹⁹R. L. Headrick, I. K. Robinson, E. Vlieg, and L. C. Feldman, Phys. Rev. Lett. **63**, 1253 (1989); P. Bedrossian, R. D. Meade, K. Mortensen, D. M. Chen, J. A. Golovchenko, and D. Vanderbilt, *ibid.* **63**, 1257 (1989); I.-W. Lyo, E. Kaxiras, and Ph. Avouris, *ibid.* **63**, 1261 (1989).

²⁰H. Hibino and T. Ogino, Phys. Rev. B **54**, 5763 (1996).

²¹N. Takeuchi, A. Selloni, and E. Tosatti, Phys. Rev. Lett. **72**, 2227 (1994).

²²A. V. Zotov, M. A. Kulakov, B. Bullemer, and I. Eisele, Phys. Rev. B **53**, 12 902 (1996).